

# Laser flash method for measuring thermal conductivity of liquids—application to low thermal conductivity liquids

Yutaka Tada, Makoto Harada, Masataka Tanigaki, and Wataru Eguchi

*Institute of Atomic Energy, Kyoto University, Uji, Kyoto, Japan*

(Received 16 November 1977; in final form, 30 May 1978)

A laser flash method developed for the measurement of thermal conductivity of solids was applied to liquids of low thermal conductivity. The sample liquid was sandwiched in between a small thin metal disk and a sample holder. When the laser beam is absorbed in the front surface of the metal disk, the temperature of the disk quickly rises about 2 K and heat then flows downwards through the sample liquid as one-dimensional heat flow. The thermal conductivity of liquid can be obtained from the temperature fall of the disk without employing any reference materials and also without measuring the thickness of the sample liquid layer. Thermal conductivities of water and toluene near room temperature were measured by this method with a mean deviation of 2.6%. This laser flash method may be applied to the measurement of the thermal conductivity of liquids such as molten salts at elevated temperatures.

## INTRODUCTION

The thermal conductivity of liquids is one of the most important transport properties, especially at elevated temperatures. There are a number of presently existing methods, steady state and transient. In steady state methods, the thermal conductivity is determined from the steady temperature gradient in the sample liquid and usually a large amount of liquid is used. It is then difficult to avoid the effect of thermal disturbances especially at elevated temperatures. Therefore, a long period of time is required in order to determine the thermal conductivity precisely and convection is liable to occur.

In case of transient methods, the time for measurement is much shorter than that in steady state methods. The hot wire method<sup>1</sup> and the flat plate stepwise heating method<sup>2</sup> are representative among transient methods. In the hot wire method, a fine wire serving as the electrical heater is embedded in a closed cylinder filled with sample liquid. The thermal conductivity of the liquid is determined from the temperature rise of the wire. Since the amount of the sample liquid is not usually small, thermal disturbances make it difficult to keep the liquid at uniform temperature before measurement, and convection is liable to occur. Further, due to the geometry employed in this method, convection in the sample liquid cannot be avoided during the measurement. The thermal conductivity could be determined in the period before convection occurs. This, however, is subject to error in determining the time when convection begins to occur.

In the flat plate stepwise heating method, the flat plate above the sample liquid is heated by electric current in stepwise fashion and the thermal conductivity of the liquid is determined from the liquid temperature rise. This method can avoid the difficulties mentioned

in the hot wire method. Since the sample liquid used is usually small in quantity in this method, the temperature of the liquid can be kept uniform before measurement. Further, as the upper part of the liquid is heated and the time for measurement is very short, convection is unlikely to occur. However, the Joule heating used in this method as well as in the hot wire method causes significant error for liquids of high electrical conductivities.

The flash method proposed by Parker *et al.*<sup>3</sup> has widely been employed as a convenient method of measuring thermal diffusivities of solid specimens. In most recent studies, a laser beam has been used as the heat source because a high energy heat pulse of very short duration can be generated. The laser beam energy is absorbed in the front surface of the solid sample and the temperature response of the back surface gives the thermal diffusivity. This is considered to be a desirable method for liquid materials at elevated temperatures, because the effect of convective heat transport can be minimized as well as in the flat plate stepwise heating method by using a horizontally mounted specimen of a very thin layer, by heating the upper part of the liquid, and by measuring a very short time temperature response. Further, this method can be applied to liquids of high electrical-conductivity such as molten salts because it does not use electric current but uses a light beam as the heat source.

The laser flash method was applied to liquid mercury by Schriempf.<sup>4</sup> The liquid mercury is in a container of an insulating material and the surface of the liquid is covered with a transparent plate of quartz. Schriempf measured the temperature rise of the back surface of the liquid as in Parker's method.

A difficulty arises, however, when Schriempf's method is to be applied to liquids of low thermal conductivity such as molten salts. Since the thermal

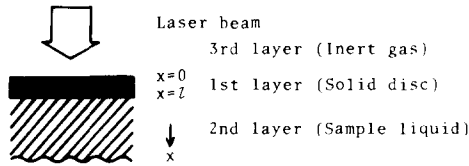


FIG. 1. Schematic diagram of the geometry of the three-layer sample.

conductivity of these liquids is of the same order as that of any available materials serving as the liquid container, heat current through the container can not be neglected. As the result, heat flow is not one-dimensional but becomes more complex. It would be necessary for the precise determination of the thermal conductivity of these liquids to avoid mathematical complexity by the use of an appropriate specimen geometry.

The aim of the present work is to apply the laser flash method to liquids of low thermal conductivity with the use of an appropriate sample geometry in order to avoid the above difficulty. The sample liquid is not surrounded by the container but is sandwiched in between a metal disk which receives the laser beam energy and a sample holder. The liquid layer is regarded as semi-infinite in order to avoid the mathematical complexity. The thermal conductivity of the liquid is determined from the measurement of the temperature fall of the front surface of the metal disk, that is, the measurement of the heat discharge into the liquid layer.

## I. THEORY

A solid opaque layer is used as shown in Fig. 1 because the laser beam passes through a transparent liquid like molten salt. The solid layer is designated as the first layer, and the liquid under and the gas above the solid layer are designated as the second and the third layers, respectively.

We postulate as follows: (1) the heat flow in question is regarded as one-dimensional. (2) The second and the third layers are regarded as semi-infinite cylindrical rods. (3) The contact resistance between the first and the second layers is neglected. (4) The physical properties

are independent of temperature because the temperature differences are small enough.

Then, the thermal diffusion equations are expressed as in Eqs. (1)–(3), and the initial and the boundary conditions are expressed as in Eqs. (4)–(10).

$$\frac{\partial T_1(x,t)}{\partial t} = \alpha_1 \frac{\partial^2 T_1(x,t)}{\partial x^2}, \quad (1)$$

$$\frac{\partial T_2(x,t)}{\partial t} = \alpha_2 \frac{\partial^2 T_2(x,t)}{\partial x^2}, \quad (2)$$

$$\frac{\partial T_3(x,t)}{\partial t} = \alpha_3 \frac{\partial^2 T_3(x,t)}{\partial x^2}. \quad (3)$$

Initial conditions,

$$T_1(x,0) = T_2(x,0) = T_3(x,0) = 0. \quad (4)$$

Boundary conditions,

$$-\lambda_1 \left. \frac{\partial T_1}{\partial x} \right|_{x=0} = f(t) - \lambda_3 \left. \frac{\partial T_3}{\partial x} \right|_{x=0}, \quad (5)$$

$$-\lambda_1 \left. \frac{\partial T_1}{\partial x} \right|_{x=l} = -\lambda_2 \left. \frac{\partial T_2}{\partial x} \right|_{x=l}, \quad (6)$$

$$T_1(0,t) = T_3(0,t), \quad (7)$$

$$T_1(l,t) = T_2(l,t), \quad (8)$$

$$T_3(-\infty, t) = 0, \quad (9)$$

$$T_2(\infty, t) = 0, \quad (10)$$

where  $t$  is time,  $x$  is the distance measured downwards from the front surface of the first layer.  $T_i(x,t)$ ,  $\lambda_i$ , and  $\alpha_i$  are the temperature rise, the thermal conductivity, and the thermal diffusivity of the  $i$ th layer, respectively, and  $f(t)$  is the function which expresses the input energy absorbed in a front unit surface of the first layer. Solving the above equations, the three temperature rises are expressed as

$$\frac{T_i(x,t)}{T_0} = \int_0^t \tilde{f}(t-\tau) F_i(x,\tau) d\tau, \quad i = 1 \sim 3, \quad (11)$$

$$F_1(x,\tau) = \frac{1}{\pi^{1/2}} \left( \frac{l^2}{\alpha_1 \tau} \right)^{1/2} \sum_{n=0}^{\infty} \left[ \frac{1}{1-H_2} \left( \frac{1-H_1}{1+H_1} \right)^{n+1} \left( \frac{1-H_2}{1+H_2} \right)^{n+1} \exp\left(-\frac{\{2(n+1)l-x\}^2}{4\alpha_1 \tau}\right) + \frac{1}{1+H_2} \left( \frac{1-H_1}{1+H_1} \right)^n \left( \frac{1-H_2}{1+H_2} \right)^n \exp\left(-\frac{(2nl+x)^2}{4\alpha_1 \tau}\right) \right], \quad (12)$$

$$F_2(x,\tau) = \frac{1}{\pi^{1/2}} \left( \frac{l^2}{\alpha_1 \tau} \right)^{1/2} \frac{2}{(1+H_1)(1+H_2)} \sum_{n=0}^{\infty} \left[ \left( \frac{1-H_1}{1+H_1} \right)^n \left( \frac{1-H_2}{1+H_2} \right)^n \exp\left(-\frac{1}{4\tau} \left\{ \frac{(2n+1)l}{\alpha_1^{1/2}} + \frac{x-l}{\alpha_2^{1/2}} \right\}^2 \right) \right], \quad (13)$$

$$F_3(x,\tau) = \frac{1}{\pi^{1/2}} \left( \frac{l^2}{\alpha_1 \tau} \right)^{1/2} \sum_{n=0}^{\infty} \left[ \frac{1}{1-H_2} \left( \frac{1-H_1}{1+H_1} \right)^{n+1} \left( \frac{1-H_2}{1+H_2} \right)^{n+1} \exp\left(-\frac{1}{4\tau} \left\{ \frac{2(n+1)l}{\alpha_1^{1/2}} - \frac{x}{\alpha_3^{1/2}} \right\}^2 \right) + \frac{1}{1+H_2} \left( \frac{1-H_1}{1+H_1} \right)^n \left( \frac{1-H_2}{1+H_2} \right)^n \exp\left(-\frac{1}{4\tau} \left\{ \frac{2nl}{\alpha_1^{1/2}} - \frac{x}{\alpha_3^{1/2}} \right\}^2 \right) \right], \quad (14)$$

where

$$H_1 \equiv \left( \frac{\lambda_2 \rho_2 c_{p2}}{\lambda_1 \rho_1 c_{p1}} \right)^{1/2}, \quad (15a)$$

$$H_2 \equiv \left( \frac{\lambda_3 \rho_3 c_{p3}}{\lambda_1 \rho_1 c_{p1}} \right)^{1/2}, \quad (15b)$$

$$T_0 \equiv \frac{Q}{\rho_1 c_{p1} l}, \quad (16)$$

$$\tilde{f}(t) \equiv \frac{f(t)}{Q}, \quad (17)$$

$$Q \equiv \int_0^\infty f(t) dt, \quad (18)$$

$c_{pi}$  and  $\rho_i$  are the specific heat capacity and the density of the  $i$ th layer, respectively.  $Q$  is the total energy absorbed in the first layer.  $T_0$  is the temperature defined by Eq. (16). Temperature responses at  $x = 0$  and  $l$  are expressed as

$$\frac{T_1(0,t)}{T_0} = \int_0^t \tilde{f}(t-\tau) F_1(0,\tau) d\tau, \quad (19a)$$

$F_1(0,\tau)$

$$= \frac{1}{\pi^{1/2}} \left( \frac{l^2}{\alpha_1 \tau} \right)^{1/2} \left[ \frac{1}{1+H_2} + \frac{2}{(1-H_2)(1+H_2)} \right] \times \sum_{n=1}^{\infty} \left( \frac{1-H_1}{1+H_1} \right)^n \left( \frac{1-H_2}{1+H_2} \right)^n \exp\left(-\frac{n^2 l^2}{\alpha_1 \tau}\right), \quad (19b)$$

$$\frac{T_1(l,t)}{T_0} = \int_0^t \tilde{f}(t-\tau) F_1(l,\tau) d\tau, \quad (20a)$$

$F_1(l,\tau)$

$$= \frac{1}{\pi^{1/2}} \left( \frac{l^2}{\alpha_1 \tau} \right)^{1/2} \frac{2}{(1+H_1)(1+H_2)} \sum_{n=0}^{\infty} \left( \frac{1-H_1}{1+H_1} \right)^n \times \left( \frac{1-H_2}{1+H_2} \right)^n \exp\left[-\frac{(2n+1)^2 l^2}{4\alpha_1 \tau}\right]. \quad (20b)$$

In the early stage of time progression, these equations can be approximated as

$$\frac{T_1(0,t)}{T_0} = \frac{1}{\pi^{1/2}} \cdot \frac{1}{1+H_2} \int_0^t \left( \frac{l^2}{\alpha_1 \tau} \right)^{1/2} \tilde{f}(t-\tau) d\tau, \quad (21a)$$

when

$$\frac{\alpha_1 t}{l^2} \ll \ln \left[ \left( \frac{1+H_1}{1-H_1} \right) \left( \frac{1+H_2}{2} \right) \right]. \quad (21b)$$

$$\frac{T_1(l,t)}{T_0} = \frac{2}{\pi^{1/2}} \cdot \frac{1}{(1+H_1)(1+H_2)} \int_0^t \left( \frac{l^2}{\alpha_1 \tau} \right)^{1/2} \times \exp\left(-\frac{l^2}{4\alpha_1 \tau}\right) \tilde{f}(t-\tau) d\tau, \quad (22a)$$

when

$$\frac{\alpha_1 t}{l^2} \ll 2 \ln \left[ \left( \frac{1+H_1}{1-H_1} \right) \left( \frac{1+H_2}{1-H_2} \right) \right]. \quad (22b)$$

On the other hand, at later times Eqs. (19) and (20) can

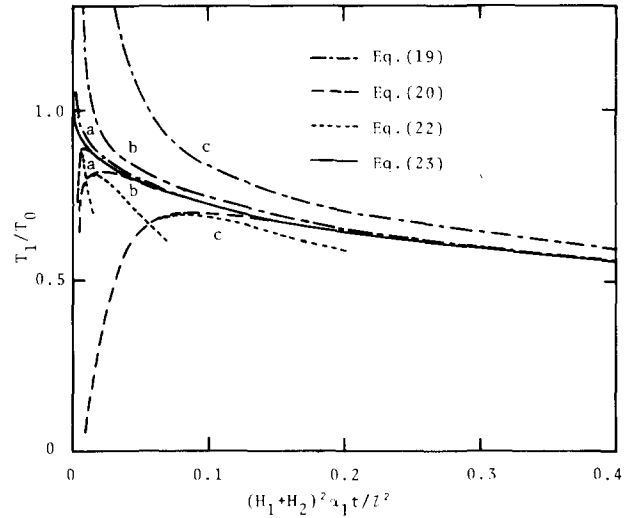


FIG. 2. Responses of the temperature change of the first layer.  $H_2 = 1.5 \times 10^{-4}$ , which corresponds to the value when the first layer is solid copper and the third is air.  $a$ ;  $H_1 = 0.1$ ;  $b$ ;  $0.2$ ;  $c$ ;  $0.4$ .

be approximated as (see Appendix A)

$$\frac{T_1(0,t)}{T_0} = \frac{T_1(l,t)}{T_0} = \exp(h^2 t) \operatorname{erfc}(ht^{1/2}), \quad (23)$$

where

$$h = h_1 + h_2, \quad (24)$$

$$h_1 \equiv \frac{(\lambda_2 \rho_2 c_{p2})^{1/2}}{\rho_1 c_{p1} l}, \quad (25a)$$

and

$$h_2 \equiv \frac{(\lambda_3 \rho_3 c_{p3})^{1/2}}{\rho_1 c_{p1} l}. \quad (25b)$$

The temperature change of the first layer,  $T_1/T_0$ , calculated from Eqs. (19), (20), (22), and (23), with  $H_1$  as the parameter, are shown in Fig. 2.  $H_2$  is fixed at  $1.5 \times 10^{-4}$  which corresponds to the value when the first layer is solid copper and the third is air. Equation (22) agrees with Eq. (20) almost up to the maximum point, regardless of  $H_1$ .

For large  $H_1$  values, the responses of the front and the back surfaces of the first layer do not agree with each other except for large values of  $\alpha_1 t/l^2$ . This indicates that the temperature of the first layer cannot be regarded as uniform.

However, when  $H_1 \leq 0.1$ , both responses agree with each other even for small values of  $\alpha_1 t/l^2$  and are expressed well by the approximate expression, Eq. (23), except in the earliest stage. This condition is satisfied for almost all liquids of low thermal conductivity.

Using Eq. (22), we can obtain the thermal diffusivity of the first layer,  $\alpha_1$ , by measuring the initial temperature rise at the back surface of it,  $T_1(l,t)$ . Using Eq. (23), we can obtain the thermal conductivity of liquid,  $\lambda_2$ , from the temperature fall of the first layer,  $T_1(0,t)$ . It should be noted that we do not need the thermal conductivity of the first layer in order to determine the thermal conductivity of the liquid from Eq. (23).

Figure 3 shows the conditions that the approximate

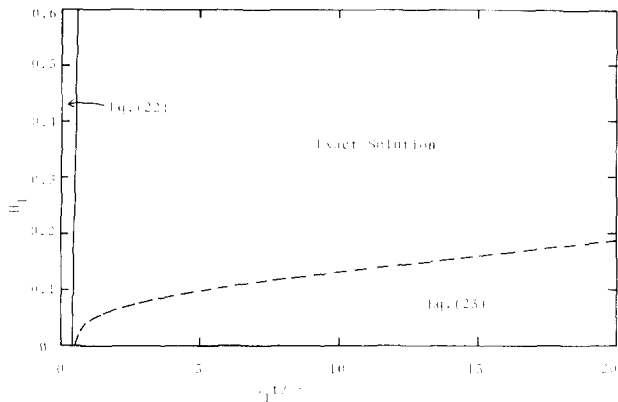


FIG. 3. Regions in which Eqs. (22) and (23) can be used, respectively, as the approximate expressions of the exact solutions Eqs. (20) and (19) within 1% error. Solid line shows the upper limit of  $\alpha_1 t/l^2$  where Eq. (22) can be used, and the broken line shows the lower limit where Eq. (23) can be used.

expressions, Eqs. (22) and (23), respectively, agree with the exact solutions (20) and (19) within 1% error. The solid line shows the upper limit of  $\alpha_1 t/l^2$ , where Eq. (22) agrees with Eq. (20) and the broken line shows the lower limit of  $\alpha_1 t/l^2$ , where Eq. (23) agrees with Eq. (19) within 1% error.

## II. EXPERIMENT

In order to realize one-dimensional heat flow as stated in the preceding chapter, liquids of low thermal conductivity cannot be surrounded by a container as used by Schriempf [Fig. 4(a)]. Instead, the sample liquid is sandwiched in between a metal disk supported horizontally by three fine wires and a lower holder as shown schematically in Fig. 4(b).

The schematic diagram of the experimental layout is shown in Fig. 5. A ruby laser with maximum energy of 3 J was used as the flash source in the present work. The beam diameter was 0.7–0.8 cm. The energy intensity of the laser beam should be uniform on the surface of the specimen. Because the laser beam used here had a hot center discussed in Schriempf's work, it was enlarged with a set of concave and convex lenses 12 with their focal lengths 15.5 and 19.0 cm, respectively and only the center part of the beam being used. The beam generated by the laser beam generator 2, after passing through the two lenses, fell onto the front surface of the metal disk in the sample cell 10. The temperature response of the metal disk was picked up by the Chromel–Alumel thermocouple 11 (0.05 mm in di-

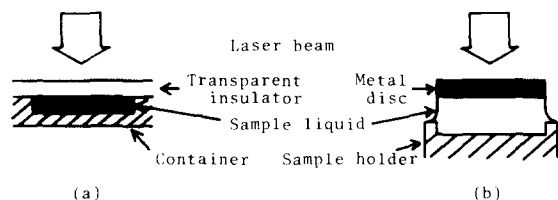


FIG. 4. Schematic diagram of the geometry of the two cells. (a) Cell used by Schriempf. Sample liquid is opaque. (b) Cell used in the present work. Sample liquid is transparent.

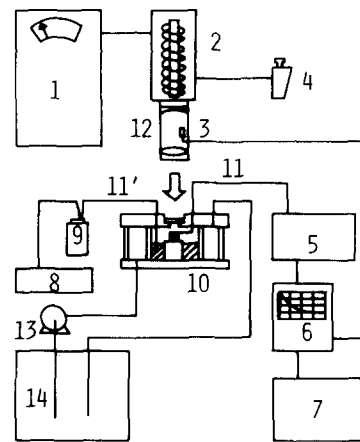


FIG. 5. Schematic diagram of the experimental layout. 1—High voltage condenser; 2—laser beam generator; 3—photodiode; 4—remote switch; 5—amplifier; 6—digital memory; 7—recorder; 8—digital voltmeter; 9—ice jar; 10—sample cell; 11,11'—thermocouple; 12—concave and convex lenses; 13—pump; 14—constant temperature bath.

ameter) spot-welded on the metal surface and was amplified by the amplifier 5 and stored in the digital memory 6. The stored response was reproduced on the chart of the recorder 7. The photodiode 3 placed between the two lenses was used as the source of the external trigger of the digital memory. The digital memory had a pretrigger circuit so that the temperature before the triggering could be recorded. The zero time was selected at the peak of the trigger pulse in the case where the temperature response of the back surface of the metal disk was measured. In the case of the temperature response of the front surface, on the other hand, the peak of the temperature jump was chosen to be zero time. The temperature response was measured as the difference from the reference temperature observed before triggering. The voltage readings on the recorder chart were exactly proportional to the electromotive force of the thermocouple. The temperature of the liquid was measured by another Chromel–Alumel thermocouple 11'. Water from a constant temperature bath 14 circulated around the cell to control the cell temperature.

Figure 6 shows the sample cell in detail. The metal disk *a* was suspended horizontally by three wires of 0.05 mm diameter. Two of them were used as the thermocouple. The sample liquid *c* was fed by the sample feeder *f* to the space (1–2 mm in depth) between the metal disk and a brass sample holder *d*. The same liquid was also poured from the feeder into the sample reservoir *c'* so that the air in the cell became saturated with the vapor of the liquid. The cell was sealed with a glass cylinder *g* and two brass disks *i* and an optical glass disk *e* through which the laser beam passed.

The thermal diffusivity of the first layer,  $\alpha_1$ , should be large and its thickness, *l*, should be small so that Eq. (23) can be used at quite early times for the measurement of the thermal conductivity of liquids. In the present case, a solid copper disk of 0.0247 cm in thickness was used as the first layer and the

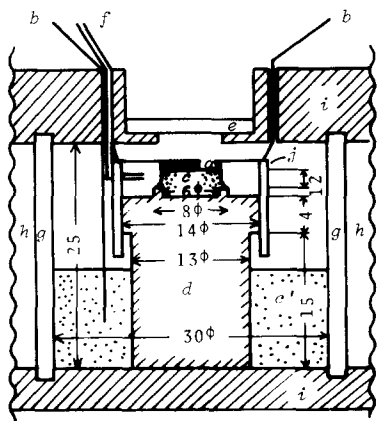


FIG. 6. Sample cell. *a*—metal disc; *b, b'*—thermocouple; *c, c'*—sample liquid; *d*—sample holder; *e*—optical glass; *f*—sample feeder; *g*—glass cylinder; *h*—water bath; *i*—brass disk; *j*—supporter (three rods welded around the sample holder in order to support three wires).

temperature response of the front surface of the copper disk was measured. The thermal diffusivity of copper need not be measured to determine the thermal conductivity of the liquid as stated in the preceding section.

For liquid samples, water and toluene were adopted. Water used was purified by distillation in an alkaline potassium permanganate solution. Toluene was of guaranteed grade (Merck Co. Ltd., purity min. 99.7%, water max. 0.0005%, nonvolatile matter max. 0.0005%).

To measure the characteristics of the laser beam, the thermal diffusivity of a standard solid material was measured without any liquid. In this case, the temperature response of the back surface of the specimen was selected. Electrolytic iron which was guaranteed by the National Bureau of Standards (U.S.) was used as the standard material.

### III. RESULTS AND DISCUSSION

#### A. Transient intensity of the laser beam

The energy intensity of the laser beam was measured with a photodiode, and its transient curve is shown in Fig. 7. The wave form can be approximated by the triangle whose area is equal to the total energy input as shown in the figure. Then,

$$\bar{f}(t) = \begin{cases} \frac{2}{t_0} \left(1 - \frac{t}{t_0}\right), & 0 < t \leq t_0 \\ 0, & t > t_0 \end{cases} \quad (26)$$

where  $t_0 = 0.822$  ms.

#### B. Measurement of the thermal diffusivity of the solid metal

The thermal diffusivity of the solid metal disk can be obtained with the help of Eq. (22) from the temperature rise at the back surface of the disk. In this case, the metal disk made contact with air only and  $H_1$  is equal to  $H_2$  in Eq. (22).

$$H_1 = H_2 = \left( \frac{\lambda_3 \rho_3 c_{p3}}{\lambda_1 \rho_1 c_{p1}} \right)^{1/2}, \quad (1 \text{—metal, } 3 \text{—air}). \quad (27)$$

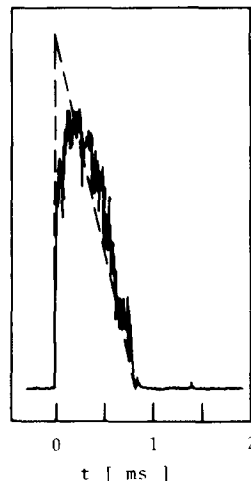


FIG. 7. Transient curve of the energy intensity of the laser beam. Broken line shows the approximate triangle wave.

The Taylor expansion of Eq. (22), neglecting higher order terms, gives (see Appendix B)

$$g(t) = \frac{2}{\pi^{1/2}} \cdot \frac{T_0}{(1 + H_2)^2} \left( \frac{t^2}{\alpha_1} \right)^{1/2} \exp\left( -\frac{t^2}{4\alpha_1 t} \right), \quad (28a)$$

where

$$g(t) \equiv T_1(l, t) t^{1/2} \left[ 1 + \frac{t_0}{3t} \left( \frac{1}{2} - \frac{t^2}{4\alpha_1 t} \right) \right]^{-1}. \quad (28b)$$

The value of  $\alpha_1$  can be obtained from the slope of the line of  $\ln g(t)$  against  $t^2/t$  by an iterative process.  $T_0/(1 + H_2)^2$  can also be obtained from the intercept. Usually two or three iterations were sufficient to obtain the converged value of  $\alpha_1$  and  $T_0/(1 + H_2)^2$ , because the second term in the denominator of Eq. (28b) was considerably smaller than the first term, unity, except at early times.

An example of the response of the temperature rise observed at the back surface of the electrolytic iron (0.0935 cm in thickness) without any liquid is shown in Fig. 8 as open circles. The temperature rise became saturated as time elapsed and it was constant after 22 ms. This suggests that the heat loss to the air layers above and below the metal disk was negligibly small for this

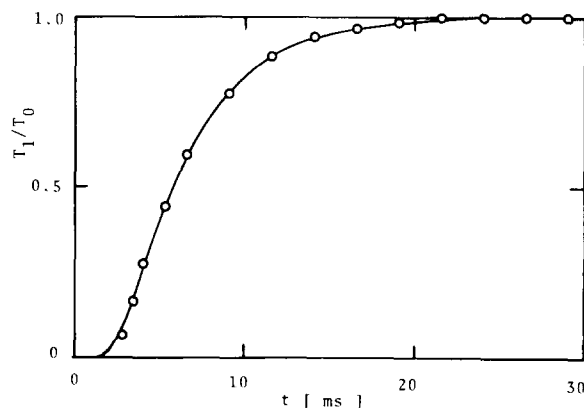


FIG. 8. Response of the temperature rise at the back surface of the electrolytic iron (0.0935 cm thick and 0.650 cm diameter). Open circles show the observed response and the solid line shows the calculated one.

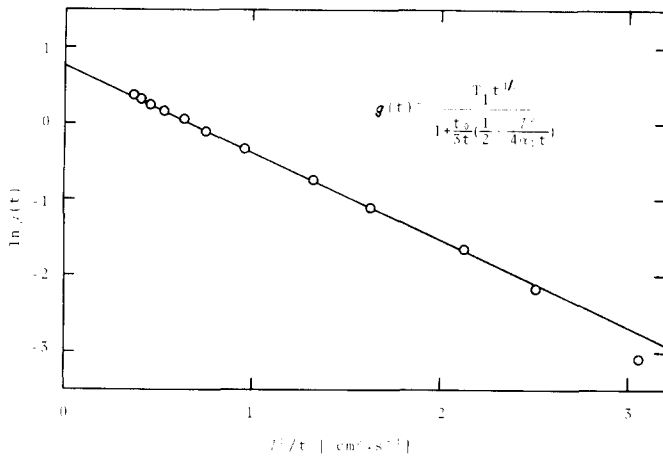


FIG. 9.  $\ln(g(t))$  against  $l^2/t$ . Slope and intercept show  $-l^2/4\alpha_1$ , and

$$\ln\left[\frac{2}{\pi^{1/2}} \cdot \frac{T_0}{(1 + H_2^2) \alpha_1}\right], \text{ respectively.}$$

sample, that is,  $H_2 = 0$ . The temperature response in Fig. 8 is normalized with this constant temperature.

Figure 9 shows the final plot of  $\ln(g(t))$  against  $l^2/t$  for the response observed in Fig. 8. After two trials,  $\alpha_1$  converged to  $0.220 \text{ cm}^2 \text{ s}^{-1}$  as shown by the straight line in the figure.  $T_0$  from the intercept agreed well with the experimental value, which confirms that the heat loss to the surrounding air is negligible.

The solid line in Fig. 8 shows the calculated response according to Eq. (20) with  $\alpha_1$  obtained above. The calculated response fits the observed one almost completely. The thermal conductivity of the electrolytic iron obtained from this experiment is  $0.787 \text{ W cm}^{-1} \text{ K}^{-1}$  at  $26.5^\circ\text{C}$ .<sup>6</sup> This agrees well with the value  $0.770 \text{ W cm}^{-1} \text{ K}^{-1}$  interpolated from the recommended values of the National Bureau of Standards. The reproducibility of the data from repeated measurements is within  $\pm 0.5\%$  error. This confirms the uniformity of the laser beam intensity on the metal surface and the one-dimensional heat flow as for the metal disk.

In the conventional laser flash method,  $\alpha_1$  is determined from the following simple relation corrected by Taylor and Cape<sup>7</sup> taking account of the finite pulse time effect:

$$\alpha_1 = l^2/\pi^2 t_c, \quad (29)$$

where  $t_c$  is the characteristic rise time of the back surface temperature. When the pulse time is infinitesimal,  $t_c = t_{1/2}/1.37$  and Eq. (29) becomes the following equation proposed by Parker *et al.*<sup>3</sup>:

$$\alpha_1 = 1.37l^2/\pi^2 t_{1/2}, \quad (30)$$

where  $t_{1/2}$  is the time required for the back surface temperature of the metal disk to reach the half of the maximum value (half time). In this work,  $t_c = t_{1/2}/1.43$  from Fig. 1 in Taylor and Cape's work<sup>7</sup> with the finite pulse time taken into consideration. Using Eq. (29), the thermal diffusivity and the conductivity of electrolytic iron were calculated to be  $0.222 \text{ cm}^2 \text{ s}^{-1}$  and

$0.795 \text{ W cm}^{-1} \text{ K}^{-1}$ , respectively, with the reproducibility within  $\pm 0.9\%$ .

The method employed in the present work, where  $\alpha_1$  was determined using the entire response curve, gave the value of  $\alpha_1$  closer to the recommended one with a better reproducibility than the half time method.

### C. Measurement of the thermal conductivity of liquid

The thermal conductivity of a liquid was obtained from the response of the front surface of the metal disk.

Figure 10 shows two examples of the temperature response of the copper disk ( $0.650 \text{ cm}$  diameter and  $0.0247 \text{ cm}$  thick). The upper curve is without liquid layer below the metal disk and the lower one with distilled water as the sample liquid. The difference of the two curves arose from the heat discharge into the water.

The upper curve decreases gradually with time. This indicates that the heat loss to the surroundings is not negligible, though it is of minor importance. In case of the measurement of the thermal diffusivity of the metal disk, electrolytic iron,  $t/l^2$  was small,  $3.43 \text{ s cm}^{-2}$  (measuring time  $t$  was within  $30 \text{ ms}$ , and the thickness of the disk  $l$  was  $0.0935 \text{ cm}$ ), that is, the response was in the early stage of time progression. The approximate equation used was Eq. (28) and the effect of heat loss was through  $H_2 = (\lambda_3 \rho_3 c_{p3} / \lambda_1 \rho_1 c_{p1})^{1/2} = 3.3 \times 10^{-4}$ , which was negligibly small compared with unity. However, in the present case,  $t/l^2$  is large,  $820 \text{ s cm}^{-2}$  ( $t = 500 \text{ ms}$  and  $l = 0.0247 \text{ cm}$ ), that is, the response is in the stage where the approximate equation, Eq. (23), is applicable. Equation (23) means that the  $h$  value is the sum of  $h_1$  and the heat loss term  $h_2$ . In this case,  $h_2$  is of the order  $10^{-3} \text{ s}^{-1/2}$  and then it is not always negligible compared with  $h_1$ .

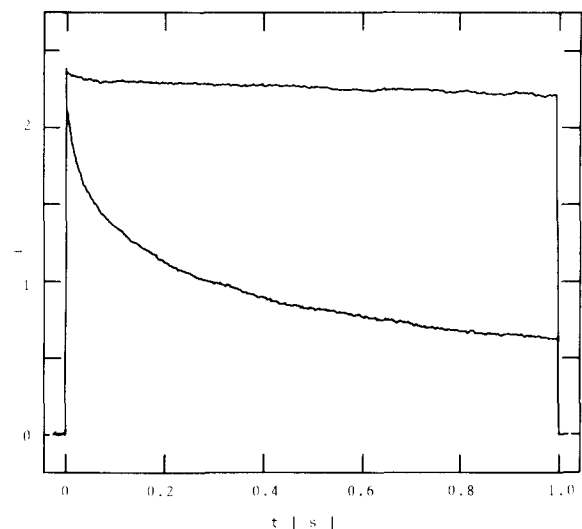


FIG. 10. Temperature responses of the front surface of the copper disk ( $0.650 \text{ cm}$  diameter and  $0.0247 \text{ cm}$  thick). Upper curve is without liquid layer below the copper disk and the lower one with distilled water as sample liquid.

## 1. Estimation of the heat loss from the metal disk

The heat loss as shown in Fig. 10 arises from heat conduction by the air layers and by the thermocouple wires, natural convection in the air, and from radiation.

The heat loss was measured when the copper disk was suspended with three, five, or six wires welded at the front surface of the disk. In all cases two of the wires were used as thermocouple. The heat loss was nearly the same. This indicates that the heat conduction through the wires is of negligible order.

Let us assume, for simplicity, that the heat transfer due to both conduction and natural convection by air can be regarded as an effective conduction process. Postulating that the conduction from the periphery of the metal disk is neglected and that the temperature difference between the disk and the surroundings is constant because the temperature fall is small, the temperature response of the disk is given as

$$\frac{T_1(t)}{T_0} = \exp(h_e^2 t) \operatorname{erfc}(h_e t^{1/2}) + \frac{1}{h_e^2} \left( 1 - \exp(h_e^2 t) \operatorname{erfc}(h_e t^{1/2}) - \frac{2}{\pi^{1/2}} h_e t^{1/2} \right) \frac{q}{\rho_1 c_{p1} l T_0}, \quad (31)$$

where  $q$  is the heat loss via radiation and  $h_e$  shows the effective heat conduction.  $h_e$  is equal to  $2h_2$  since the disk has two faces, the front and the back surfaces. Then,

$$h_e = 2h_2 = 2(h_{cd} + h_{cv}), \quad (cd\text{---conduction, } cv\text{---convection}), \quad (32a)$$

$$h_{cd} = (\lambda_3 \rho_3 c_{p3})^{1/2} / \rho_1 c_{p1} l, \quad (1\text{---metal, } 3\text{---air}). \quad (32b)$$

The heat loss shown in Fig. 10 is small and the order of  $h_e$  is sufficiently small. Then Eq. (31) can be approximated as follows by neglecting higher order terms of  $h_2$ :

$$\frac{T_1(t)}{T_0} = 1 - \frac{4}{\pi^{1/2}} h_2 t^{1/2} - \frac{q}{\rho_1 c_{p1} l T_0} t. \quad (33)$$

In the present experiments, the metal disk was made of copper,  $T_0$  was about 2 K and the time of measurement was shorter than 500 ms. The second term of the right hand side of Eq. (33) is bigger than  $1.2 \times 10^{-2}$  which was estimated with the effect of natural convection neglected. The third term is smaller than  $1.1 \times 10^{-4}$  which was calculated for the case that the disk was completely surrounded by a blackbody. The second term is much larger than the third. Then, Eq. (33) can safely be approximated as

$$T_1(t)/T_0 = 1 - (4/\pi^{1/2}) h_2 t^{1/2}. \quad (34)$$

Figure 11 shows the plot of  $T_1$  against  $t^{1/2}$  ( $t < 500$  ms) when the disk was suspended with three wires. From the average slope of these straight lines,  $h_2$  is determined to be  $0.018 \text{ s}^{-1/2}$ .<sup>8</sup> The heat loss was also evaluated

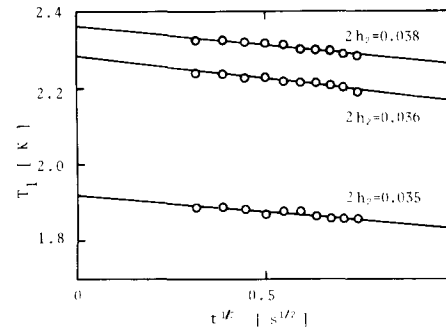


FIG. 11.  $T_1$  against  $t^{1/2}$  ( $t < 500$  ms). Slope and intercept show  $-4h_2 T_0 / \pi^{1/2}$  and  $T_0$ , respectively.

as  $h_2$  when five or six wires were welded as mentioned above. In the former case  $h_2 = 0.018 \text{ s}^{-1/2}$  and in the latter  $h_2 = 0.012 \text{ s}^{-1/2}$ . There is no tendency that  $h_2$  value increases with increasing the number of the wires. It can be said that the heat loss via wire conduction is negligibly small.

## 2. Determination of the thermal conductivity of liquid

In this work, the total input energy  $Q$  is different for each experimental run because of the subtle difference of the bead placement and that of the surface state of the disk (reflectivity and absorptivity).  $T_0$  and  $\lambda$  were determined simultaneously from the temperature response curve for each experimental run.

The values of  $h$  and  $T_0$  obtained were  $1.917 \text{ s}^{-1/2}$  and  $2.38 \text{ K}$ , respectively; this was accomplished by fitting Eq. (23) to the response curve of Fig. 10 in the range of  $10 < t < 500$  ms with the least-squares method.  $h_1$  is determined by subtracting  $h_2$  obtained with Eq. (34) from  $h$ . From  $h_1$ , the thermal conductivity of liquid,  $\lambda_2$ , is obtained with the use of the values of  $\rho_1 l$ ,  $c_{p1}$ ,  $\rho_2$ , and  $c_{p2}$ .<sup>9</sup> The value of  $\lambda_2$  obtained at the condition in Fig. 10 was  $6.07 \times 10^{-3} \text{ W cm}^{-1} \text{ K}^{-1}$  ( $21.3^\circ\text{C}$ ). Since  $\alpha_1$  is estimated to be about  $1.1 \text{ cm}^2 \text{ s}^{-1}$ , the value of  $H_1$  for this value of  $\lambda_2$  is 0.045, and then Eq. (23) can safely be used from the early stage,  $\alpha_1 t / l^2 > 1$ , i.e.  $t > 0.6$  ms from Fig. 3.

The temperature response of the copper-water system in Fig. 10 where  $10 \text{ ms} < t < 1 \text{ s}$  was replotted in Fig. 12. The ordinate in Fig. 12 is scaled such that the relation between  $T_1/T_0$  and  $t^{1/2}$  gives a straight line according to Eq. (23). The solid line was the relation calculated by Eq. (23) with the  $h$  value obtained above. The plotted points show  $T_1/T_0$  against  $t^{1/2}$  with the observed values of  $T_1$  with  $T_0$  obtained by the least-squares method. They agree very well with the calculated one.

The measured thermal conductivities of water and of toluene are shown in Figs. 13 and 14 together with some of the previously published data. The former agree well with the latter.

The convection in liquid is one of the serious sources of error in the measurement of the thermal conductivity of liquid and much attention should be paid to avoid it. In the present experiments, the sample liquid was thin enough and the temperature difference between the top

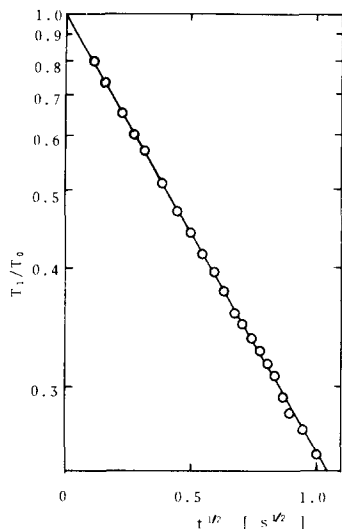


FIG. 12. Temperature response of copper-water system. Open circles show  $T_1/T_0$  against  $t^{1/2}$  with  $T_1$  observed and  $T_0$  obtained by the least-squares method. Solid line shows the relation between the right hand side of Eq. (23) and  $t^{1/2}$ .

and the bottom of the sample liquid was only about 2 K. Rayleigh number  $Ra$  was 730 and  $Ra \cdot d = 220$  cm ( $d$  is the liquid thickness in cm), which is much less than  $5 \times 10^4$  cm where the heat transfer via convection becomes 1% of that via conduction when the angle of the liquid layer with the horizontal plane does not exceed  $0.04^\circ$ .<sup>10</sup> Furthermore, the measuring time was very short, some hundreds of milliseconds. Therefore, it can safely be said that the convection is negligible during the measuring time.

The evaporation of the sample liquid during the measuring time would be neglected because the system was sealed and the maximum temperature rise of the metal disk was only about 2 K and the saturated vapor pressure of the sample liquid was much less than the total pressure in the cell, which is equal to the atmospheric pressure.

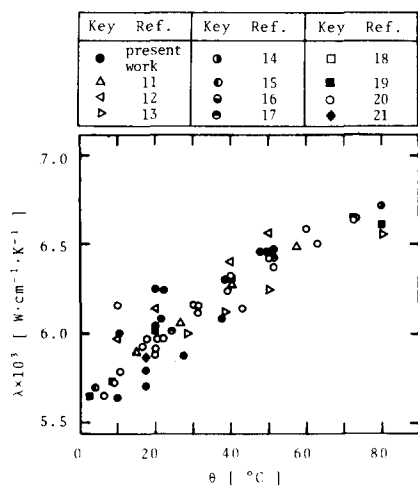


FIG. 13. Thermal conductivities of water. Meyer and Eigen,<sup>11</sup> Martin and Lang,<sup>12</sup> Nukiyama,<sup>13</sup> Van der Held, Hardebol, and Kalshoven,<sup>14</sup> Gillam and Lamm,<sup>15</sup> Dick and Mckready,<sup>16</sup> Challoner and Powell,<sup>17</sup> Schmidt and Sellshop,<sup>18</sup> Riedel,<sup>19</sup> Schmidt and Leidenfrost,<sup>20</sup> Yamamoto and Akiyama.<sup>21</sup>

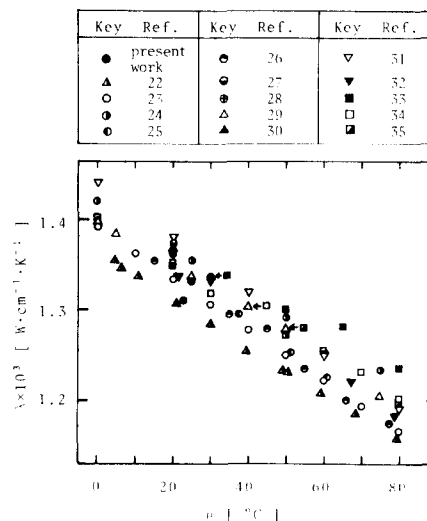


FIG. 14. Thermal conductivities of toluene. Tree and Leidenfrost,<sup>22</sup> Venert,<sup>23</sup> Usmanov and Mukhamedzyanov,<sup>24</sup> Horrocks and McLaughlin,<sup>25</sup> Ziebland,<sup>26</sup> El'darov,<sup>27</sup> Frontas'ev and Gusakov,<sup>28</sup> Os'minin,<sup>29</sup> Briggs,<sup>30</sup> Challoner and Powell,<sup>31</sup> Schmidt and Leidenfrost,<sup>32</sup> Filippov,<sup>33</sup> Vargaftik,<sup>34</sup> Riedel.<sup>35</sup>

The temperature response of the first layer obeys Eq. (23), which is derived based on one-dimensional heat flow, and the observed thermal conductivities agree well with the previously published data, and further, convection in liquid and evaporation can be neglected. These confirm that the heat flow can be regarded as one-dimensional and that the thermal conductivity of liquid can be determined with this laser flash method. The mean deviation of these data is 2.6%.

In this work, the basic measurements were done almost exactly and the error of the results is mainly attributed to the exactness of the one-dimensionality due to the difference of the shape of the cylindrical sample liquid. It is quite difficult to estimate this exactness and thus the sensitivity of the results to it quantitatively. It can only be said that the reproducibility was within 2.6% error and the one-dimensionality was satisfied at least within this error.

The mean deviation is slightly larger than that of carefully performed steady state methods. However, in steady state methods, heat flux should be measured directly to obtain the thermal conductivity absolutely and it is quite difficult to estimate the heat loss. Therefore, most of the steady state methods are relative methods using reference materials. In this laser flash method, heat loss via conduction and convection can be easily estimated, and the thermal conductivity of a liquid can be obtained without employing any reference materials. This is a significant advantage in measurements at elevated temperatures.

This laser flash method has the following four advantages. (1) The sample liquid is a very thin layer (1–2 mm) and little in quantity. It is easy to control the temperatures of both the sample liquid and the atmosphere and to make the liquid temperature uniform before measurement. (2) The heat loss from the sample to the surrounding gas can easily be estimated. (3) Absolute



measurement is possible for the liquids of low thermal conductivity, without measuring directly the total input energy  $Q$  and the liquid thickness. (4) The temperature rise of the sample liquid is only about 2 K, so that near room temperature the heat loss via radiation can be neglected, and even at elevated temperatures it will be small and may easily be estimated. Due to these advantages this laser flash method will be applicable to the measurement of the thermal conductivity of low thermal conductivity liquids, such as molten salts at elevated temperatures.

## ACKNOWLEDGMENTS

The authors gratefully acknowledge the financial support from a grant in aid for fundamental scientific research, Ministry of Education, Japan. The numerical calculations were carried out at Data Processing Center, Kyoto University.

## APPENDIX A

Equation (23) is the solution  $T_1(t)$  of the following thermal diffusion equations:

$$-\rho_1 c_{p1} l \frac{dT_1(t)}{dt} = \lambda_3 \left. \frac{\partial T_3}{\partial x} \right|_{x=0} - \lambda_2 \left. \frac{\partial T_2}{\partial x} \right|_{x=l}, \quad (\text{A1})$$

$$\frac{\partial T_2(x,t)}{\partial t} = \alpha_2 \frac{\partial^2 T_2(x,t)}{\partial x^2}, \quad (\text{A2})$$

$$\frac{\partial T_3(x,t)}{\partial t} = \alpha_3 \frac{\partial^2 T_3(x,t)}{\partial x^2}. \quad (\text{A3})$$

Initial conditions:

$$T_1(0) = T_0, \quad (\text{A4})$$

$$T_2(x,0) = T_3(x,0) = 0. \quad (\text{A5})$$

Boundary conditions:

$$T_1(t) = T_2(l,t) = T_3(0,t), \quad (\text{A6})$$

$$T_2(\infty, t) = 0, \quad (\text{A7})$$

$$T_3(-\infty, t) = 0. \quad (\text{A8})$$

Solving these equations, we obtain  $T_1(t)$  expressed as

$$\frac{T_1(t)}{T_0} = \exp\left(\frac{H^2 \alpha_1 t}{l^2}\right) \operatorname{erfc}\left[H\left(\frac{\alpha_1 t}{l^2}\right)^{1/2}\right] = \exp(h^2 t) \operatorname{erfc}(ht^{1/2}), \quad (\text{A9})$$

where

$$H = H_1 + H_2 \quad (\text{A10})$$

$$h = h_1 + h_2. \quad (\text{A11})$$

## APPENDIX B

When  $t$  in Eq. (26) is replaced by  $t - \tau$ , Eq. (26) becomes

$$\tilde{f}(t - \tau) = \begin{cases} \frac{2}{t_0} \left(1 - \frac{t - \tau}{t_0}\right), & 0 < t - \tau \leq t_0 \\ 0, & t - \tau > t_0. \end{cases} \quad (\text{B1})$$

Substituting Eq. (B1) into Eq. (22a), the following equation can be obtained:

$$\frac{T_1(l,t)}{T_0} = \frac{2}{\pi^{1/2}} \cdot \frac{1}{(1 + H_2)^2} \int_{t-t_0}^t \left(\frac{l^2}{\alpha_1 \tau}\right)^{1/2} \exp\left(-\frac{l^2}{4\alpha_1 \tau}\right) \times \frac{2}{t_0} \left(1 - \frac{t - \tau}{t_0}\right) d\tau. \quad (\text{B2})$$

The lower limit of the integral has been replaced by  $t - t_0$  because  $\tilde{f}(t - \tau)$  vanishes for  $\tau < t - t_0$ . Expansion of  $[l^2/(\alpha_1 \tau)]^{1/2} \exp[-l^2/(4\alpha_1 \tau)]$  in a Taylor series at time  $t$ , retaining only the first two terms leads to

$$\left(\frac{l^2}{\alpha_1 \tau}\right)^{1/2} \exp\left(-\frac{l^2}{4\alpha_1 \tau}\right) = \left(\frac{l^2}{\alpha_1 t}\right)^{1/2} \exp\left(-\frac{l^2}{4\alpha_1 t}\right) \times \left[1 + \left(-\frac{1}{2t} + \frac{l^2}{4\alpha_1 t^2}\right)(\tau - t) + \dots\right]. \quad (\text{B3})$$

Higher order terms of  $\tau - t$  do not contribute  $T_1(l,t)/T_0$  in Eq. (B2).

Substitution of Eq. (B3) into Eq. (B2) and the following integration leads to

$$\frac{T_1(l,t)}{T_0} = \frac{2}{\pi^{1/2}} \cdot \frac{1}{(1 + H_2)^2} \left(\frac{l^2}{\alpha_1 t}\right)^{1/2} \exp\left(-\frac{l^2}{4\alpha_1 t}\right) \times \left[1 + \frac{t_0}{3t} \left(\frac{1}{2} - \frac{l^2}{4\alpha_1 t}\right)\right]. \quad (\text{B4})$$

Defining  $g(t)$  as

$$g(t) \equiv T_1(l,t)t^{1/2} \left[1 + \frac{t_0}{3t} \left(\frac{1}{2} - \frac{l^2}{4\alpha_1 t}\right)\right]^{-1}, \quad (\text{B5})$$

Eq. (B4) becomes

$$g(t) = \frac{2}{\pi^{1/2}} \cdot \frac{T_0}{(1 + H_2)^2} \left(\frac{l^2}{\alpha_1}\right)^{1/2} \exp\left(-\frac{l^2}{4\alpha_1 t}\right). \quad (\text{B6})$$

- <sup>1</sup> J. K. Horrocks and E. McLaughlin, Proc. R. Soc. London **A273**, 259 (1963).
- <sup>2</sup> K. Kobayashi and N. Araki, *Heat Transfer 1974*, V (Scripta, Washington, D.C., 1974), p. 247.
- <sup>3</sup> W. J. Parker, R. J. Jenkins, C. P. Bulter, and G. L. Abbott, J. Appl. Phys. **32**, 1679 (1961).
- <sup>4</sup> J. T. Schriempf, Rev. Sci. Instrum. **43**, 781 (1972).
- <sup>5</sup> Heat penetration length in the sample liquid is about 1 mm in case of water when  $t = 1$  s. Then, we can regard the liquid layer as a semi-infinite rod when  $t < 1$  s. The response within 500 ms was analyzed to determine the thermal conductivity of liquid.
- <sup>6</sup> For  $\rho$  and  $c_p$ , the recommended values were used as follows:  $\rho$ —W. G. McMillan and A. L. Latter, J. Chem. Phys. **29**, 15 (1958).  $c_p$ —G. S. Kell and E. Whalley, Philos. Trans. **A258**, 565 (1965).
- <sup>7</sup> R. E. Taylor and J. A. Cape, Appl. Phys. Lett. **5**, 212 (1964).
- <sup>8</sup> The theoretical value of  $h_{cd}$  is  $0.007 \text{ s}^{-1/2}$ . The difference between the theoretical value of conduction and the observed value of effective conduction may be due to natural convection.
- <sup>9</sup>  $\rho_1 l$  was determined by measuring the mass of the copper disk and for the values of  $c_{p1}$ ,  $\rho_2$ , and  $c_{p2}$ , the recommended values were used as follows:  $c_{p1}$ —(Copper) *Landolt-Börnstein, Physikalisch-Chemische Tabellen, II* (1923), p. 1245.  $\rho_2$ —(Water) *Kagaku-Binran, Kisoheon II* (Chemical Society of Japan), p. 432; *Landolt-Börnstein (new Series) IV/1a*, p. 658. (Toluene) Bureau International d'Etalons Physico-Chimiques.  $c_{p2}$ —(Water) Comité International des Poids et Mesures (1950). (Toluene) N. B. Vargaftik, *Thermophysical Properties of Substances* (A Handbook, Gosenergo Press, 1956).
- <sup>10</sup> A. Michels and J. V. Sengers, Physica **28**, 1238 (1962).
- <sup>11</sup> E. Meyer and M. Eigen, Z. Naturf. **8a**, 500 (1953).
- <sup>12</sup> L. H. Martin and K. C. Lang, Proc. Phys. Soc. **45**, 523 (1933).

- <sup>13</sup> S. Nukiyama, *Kikaigakkaishi* **37**, 206 (1935).
- <sup>14</sup> E. F. M. Van der Held, J. Hardebol, and J. Kalshoven, *Physica* **19**, 208 (1953).
- <sup>15</sup> D. G. Gillam and O. L. Lamm, *Scand. Chem. Acta* **9**, 657 (1955).
- <sup>16</sup> M. F. Dick and D. W. Mcready, *Trans. Am. Soc. Mech. Eng.* **76**, 831 (1954).
- <sup>17</sup> A. R. Challoner and R. W. Powell, *Proc. R. Soc.* **A238**, 90 (1956).
- <sup>18</sup> E. Schmidt and W. Sellshop, *Forsch. Geb. Ingenieurwes.* **3**, 277 (1932).
- <sup>19</sup> L. Riedel, *Chem. Ing. Tech.* **23**, 321 (1951).
- <sup>20</sup> E. Schmidt and W. Leidenfrost, *Forsch. Ingenieurwes.* **21**, 176 (1955).
- <sup>21</sup> A. Yamamoto and J. Akiyama, *Kogyo Kagaku Zasshi*, **69**, 1659 (1966).
- <sup>22</sup> D. R. Tree and W. Leidenfrost, *Thermal conductivity, Proceedings of Eighth Conference* (Plenum, New York, 1968), p. 611.
- <sup>23</sup> J. E. S. Venert, *The International Thermal Conductivity Conference* (Teddington, Middlesex), July (1964).
- <sup>24</sup> A. G. Usmanov and G. Kh. Mukhamedzyanov, *Intern. Chem. Eng.* **3**, 369 (1963).
- <sup>25</sup> J. K. Horrocks and E. McLaughlin, *Proc. R. Soc. London* **A273**, 259 (1963).
- <sup>26</sup> H. Ziebland, *Intern. J. Heat Mass Trans.* **2**, 273 (1961).
- <sup>27</sup> F. G. El'darov, *Russ. J. Phys. Chem.* **34**, 677 (1960).
- <sup>28</sup> V. P. Frontas'ev and M. Ya. Gusakov, *Zhur. Tekh. Fiz.* **29**, 1277 (1959). *English Trans., Soviet Phys.—Tech. Phys.* **4**, 1171 (1960).
- <sup>29</sup> Yu. P. Os'Minin, *Vestn. Mosk. Univ. Ser. Mater. Mekhan. Astron. Fiz. Khim.* **12**, 117 (1957).
- <sup>30</sup> D. K. H. Briggs, *Ind. Eng. Chem.* **49**, 418 (1957).
- <sup>31</sup> A. R. Challoner and R. W. Powell, *Proc. R. Soc. London* **A238**, 90 (1956).
- <sup>32</sup> E. Schmidt and W. Leidenfrost, *Forsch. Geb. Ingenieurwes.* **19**, 65 (1953).
- <sup>33</sup> L. P. Filippov, *Vestn. Mosk. Univ. 8(9), Ser. Fiz.-Mat. Estest. Nauk* No. 6, 109 (1953). *English Trans. L.C or SLA 61-10145, 1* (1960).
- <sup>34</sup> N. B. Vargaftik and L. P. Filippov, *Thermal Conductivity of Gases and Liquids* (Standards Press, Massachusetts, 1970).
- <sup>35</sup> L. Riedel, *Arch. Tech. Messen.* **227**, 273 (1954).